BILINGUAL PUBLISHING CO.
Pioneer of Global Academics Since 1984

Journal of Computer Science Research
http://ojs.bilpublishing.com/index.php/jcsr

ARTICLE

Rectangular Body-centered Cuboid Packing Lattices and Their Possible Applications

Xiqiang Zheng*

Department of Science, Technology, Health and Human Services, Voorhees College, Denmark, SC 29042, USA

ARTICLE INFO

Article history
Received: 15 March 2019
Accepted: 28 May 2019
Published Online: 30 July 2019

Keywords:
Sphere packing
Lattices
FCC lattices
BCC lattices
Discretization

ABSTRACT

We first introduce several sphere packing ways such as simple cubic packing (SC), face-centered cubic packing (FCC), body-centered cubic packing (BCC), and rectangular body-centered cuboid packing (recBCC), where the rectangular body-centered cuboid packing means the packing method based on a rectangular cuboid whose base is square and whose height is times the length of one side of its square base such that the congruent spheres are centered at the 8 vertices and the centroid of the cuboid. The corresponding lattices are denoted as SCL, FCCL, BCCL, and recBCCL, respectively. Then we consider properties of those lattices, and show that FCCL and recBCCL are the same. Finally we point out some possible applications of the recBCC lattices.

1. Introduction

Throughout this paper, let R, Z, and N denote the set of real numbers, integers and natural numbers, respectively. For any $n \in N$ and $x_1, x_2, \ldots, x_n \in R$, the notation $(x_1, x_2, \ldots, x_n)$ denotes the coordinates of an n dimensional point or denotes an n dimensional vector depending on the context. If

u_1, u_2, …, and u_n are n linearly independent vectors in R^n, then the set

$$L = \left\{ \sum_{i=1}^{n} k_i \bullet u_i : k_i \in Z \ \ for \ i = 1, 2, \ldots, n \right\}$$

is called an n dimensional lattice generated by u_1, u_2,…, and u_n. These n vectors are called a set of generators of the lattice. An n dimensional Cartesian lattice is generated by n vectors that have the same length and are orthogonal to each other. A hexagonal lattice is a lattice generated by two vectors that have the same length and the angle between them is 120° or 60°. Figure 1 shows a hexagonal lattice and a 2-dimensional Cartesian lattice.

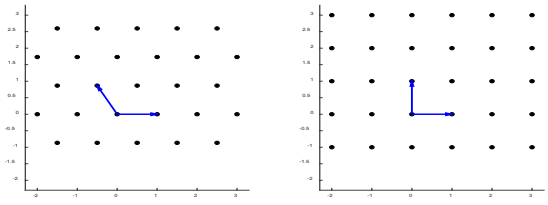

Figure 1. The left and the right show a set of generators in blue color of a hexagonal lattice and a square lattice, respectively

**Corresponding Author:*
Xiqiang Zheng,
Department of Science and Technology, Voorhees College, Denmark, SC 29042, USA;
Email: xzheng@voorhees.edu

 DOI: https://doi.org/10.30564/jcsr.v1i2.641

The usual computations are done on a Cartesian lattice for discretization of a geometric object. However optimal sampling lattices have better adjacency relation than the corresponding Cartesian lattices, and sometimes provide more efficient sampling. Each lattice point in a hexagonal lattice has six equidistant neighbors. Hexagonal lattices may be applied in image processing tasks such as reconstruction and segmentation. In [1] by Ikeda and Murota, and in [2] by Vince and Zheng, hexagonal lattices are considered for Earth mapping. In [3] by Hofmann and Tiede, hexagonal sampling grids are applied for Earth image segmentation. In [4] by Wei et al. and in [5] by Burdescu et al., graph cuts methods and hexagonal grids are applied to image segmentation. Mostafa and Her in [6] applied hexagonal grids for edge detection.

To make the application of hexagonal lattices convenient, some tools for scientific computations on hexagonal lattices have been developed. As shown in [2] by Vince and Zheng, some efficient algorithms for discrete Fourier transforms on hexagonal lattices were developed. Voronoi splines for hexagonal lattices were studied in [7] by Van De Ville et al. and in [8] by Mirzargar and Entezari. Li in [9] implemented a simulated display system for hexagonal image processing.

In this following, we first introduce some 3-dimensional sphere packing ways and related lattices. Then we consider the corresponding optimal sampling lattices and their properties. Finally, we point out some possible applications of those properties.

2. Some 3-dimensional Sphere Packing Ways and Related Lattices

As in Wikipedia webpage [10], the proportion of space filled by the spheres is called the packing density. The following are several sphere packing examples.

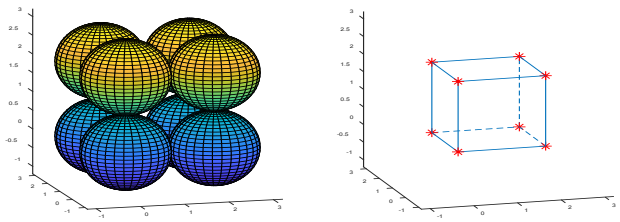

Figure 2. The left shows simple cubic packing of spheres, and the right shows the eight red star points that are the centroids of those spheres

Example 1: Simple Cubic packing introduced in Wikipedia webpage [11]. As shown in the left of Figure 2, corresponding to the simple cubic packing, spheres are stacked layer by layer such that each sphere in the second level touches and is directly above a sphere in the first layer. As shown in the right of Figure 2, the centroids of those spheres are lattice points of a cubic lattice that is generated by three vectors which are orthogonal to each other and have the same length. It is easy to verify that the packing density is $\frac{\pi}{6} \approx 52.36\%$.

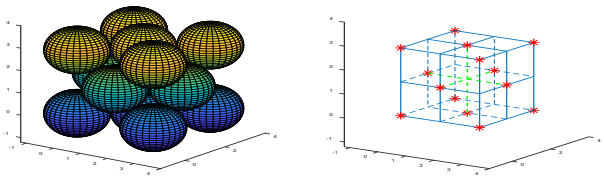

Figure 3. The left shows FCC packing of spheres, and the right shows the 14 red star points that are the centroids of those spheres

Example 2: Face-Centered Cubic packing introduced in Wikipedia webpage [11]. As shown in the left of Figure 3, corresponding to the Face-Centered Cubic packing (FCC), there are eight spheres centered at the vertices of a cube and there are six spheres whose center points are exactly the center points of the six faces of the cube. Let be the radius of the spheres in Figure 3 and let s be the length of one side of the cube shown in the right side of Figure 3. Then the length of each diagonal of a face for the cube is $4r$. Hence $s = 2\sqrt{2}\,r$.

The sphere centered at the origin has exactly $\frac{1}{8}$ of the volume enclosed in the cube because the cube is in the first octant and the volume of the sphere in each of the 8 octants is the same. For a similar reason, each sphere centered at one of the vertices of the cube in Figure 3 has exactly $\frac{1}{8}$ of the volume enclosed in the cube. The sphere centered at the centroid of one face of the cube has half of its volume enclosed in the cube. In Figure 3, there are 8 spheres centered at the 8 vertices and there are 6 spheres centered at the 6 faces of the cube. Hence the total volume of the spheres enclosed in the cube is

$$V_{spheres} = \left(8 \bullet \frac{1}{8} + 6 \bullet \frac{1}{2}\right) \bullet \frac{4\pi r^3}{3} = \frac{16\pi r^3}{3}.$$

The volume of the cube is $V_{cube} = s^3 = 16\sqrt{2} \bullet r^3$. The structure enclosed by the cube is a representative unit meaning that we get a bigger structure with the same packing density if we tessellate this structure side by side. Hence the packing density of FCC lattices is

$$\frac{V_{spheres}}{V_{cube}} = \frac{\pi}{3\sqrt{2}} \approx 74.05\%$$

.

DOI: https://doi.org/10.30564/jcsr.v1i2.641

Example 3: Body-Centered Cubic packing introduced in Wikipedia webpage [11]. Corresponding to Body-Centered Cubic packing (BCC), congruent spheres are stacked such that 8 of them are centered at the 8 vertices of a cube (shown in the right side of Figure 4) and one of them is centered at the centroid of the cube. Let s be the length of one side of the cube and assume that the cube is in the first octant with $(0,0,0)$, $(s,0,0)$, $(0,s,0)$, and $(0,0,s)$ as vertices. Then the coordinates of the centroid of the cube are $\left(\frac{s}{2},\frac{s}{2},\frac{s}{2}\right)$. It follows that the distance between the centroid and the origin is $\frac{\sqrt{3}}{2}s$. Since $\frac{\sqrt{3}}{2}s=2r$, where r is the radius of the spheres in Figure 4, we have $r=\frac{\sqrt{3}}{4}s$. Each sphere centered at the 8 vertices of the cube has $\frac{1}{8}$ volume enclosed in the cube and the sphere at the centroid of the cube is completely enclosed in the cube. Hence the total volume of the sphere enclosed in the cube is

$$V_{spheres}=\left(8\bullet\frac{1}{8}+1\right)\bullet\frac{4\pi\bullet r^3}{3}=\frac{8\pi r^3}{3}=\frac{\sqrt{3}\,\pi}{8}\bullet s^3 .$$

The volume of the cube is $V_{cube}=s^3$. Therefore the packing density of BCC lattices is

$$\frac{V_{spheres}}{V_{cube}}=\frac{\sqrt{3}\,\pi}{8}\approx 68.02\% .$$

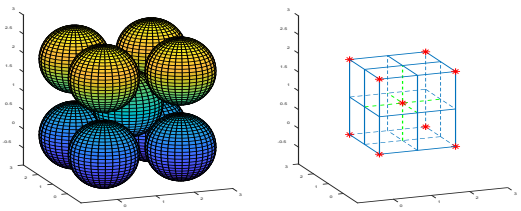

Figure 4. The left shows BCC packing of spheres, and the right shows the 9 red star points that are the centroids of those spheres

As mentioned in [12] by Kim et al., BCC lattices and FCC lattices outperform the Cartesian lattices for the reconstruction of tri-variate functions; BCC lattice are the optimal 3D sampling lattices; and FCC lattices exhibit nearly-optimal sampling properties. As displayed in [13] by Zheng and Gu, each lattice point in an FCC lattice has 12 equidistant neighbors, and the lattice has a uniform notion of voxel neighborhood. Hence FCC lattices are more suitable than 3D Cartesian lattices for morphological operations.

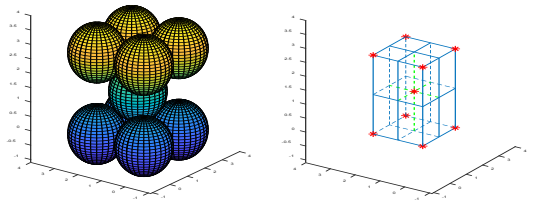

Figure 5. The left shows rectangular BCC packing of spheres, and the right shows the 9 red star points that are the centroids of those spheres

Some tools for scientific computations on FCC and BCC lattices have been developed. Fast algorithms for discrete Fourier transform on FCC and BCC lattices were studied as shown in [13] by Zheng and Gu. For FCC and BCC lattices, Voronoi splines are studied in [8] by Mirzargar and Entezari; and the box spline reconstruction for FCC lattices is studied in [12] by Kim et al. In the following, we consider another novel kind of sphere packing and its related lattices. Interestingly enough, the related lattices turn out to be the same as FCC lattices.

Example 4: Rectangular Body-Centered Cuboid packing. To explore the relation between FCC lattices and BCC lattices, in this paper, we introduce rectangular body-centered cuboid packing that is defined in the following. Consider a rectangular cuboid that has a square base and whose height is $\sqrt{2}$ times the length of one side of its square base as shown in the right side of Figure 5. As shown in the left side of Figure 5, congruent spheres are stacked such that 8 of them are centered at the 8 vertices of the cuboid and one of them is centered at the centroid of the cuboid. Because the height of the cuboid is different from the length of one side of its square base, we call this kind of stacking the rectangular Body-Centered Cuboid ($recBCC$) packing.

3. The Equivalence of FCC Lattices and Rectangular Body Centered Cuboid Packing Lattices

In this section, by considering the generators of those lattices, we show that each FCC lattice is generated by three vectors that have the same length and the angle between any two of these three vectors is 60°. So is each $recBCC$ lattice. Hence the set of FCC lattices is the same as the set of $recBCC$ lattices. In other words, $FCCL=recBCCL$ where $FCCL$ and $recBCCL$ denote the set of FCC lattices and the set of $recBCC$ lattices respectively.

 DOI: https://doi.org/10.30564/jcsr.v1i2.641

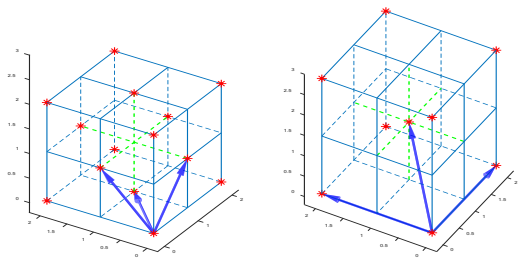

Figure 6. The left and the right show a set of generators in blue color of a BCC lattice and a rectangular BCC lattice, respectively

The FCC lattice shown in the left side of Figure 6 is generated by three vectors $u_1 = k \bullet (\sqrt{2}, 0, \sqrt{2})$, $u_2 = k \bullet (\sqrt{2}, \sqrt{2}, 0)$, and $u_3 = k \bullet (0, \sqrt{2}, \sqrt{2})$ for some scaling factor $k > 0$. Hence any FCC lattice is generated by three vectors that have the same length and the angle between any two of them is 60°. To show that the lattice displayed at the right side of Figure 6 is also such a lattice, we need some definitions as in the following.

Let a_i and b be vectors for each $i = 1, 2, ..., m$. If there exist integers k_1, k_2, ..., and k_m such that $b = \sum_{i=1}^{m} k_i \bullet a_i$, then the vector b is called an integer linear combination of a_1, a_2, …, and a_m. For two sets of vectors, if each vector in any of those two sets is an integer linear combination of the vectors in another set, then those two sets of vectors are called equivalent with respect to integer linear combinations. The following Lemma 1 shows that, if two sets of vectors are equivalent with respect to integer linear combinations, then these two sets generate the same lattice. Lemma 1 will be applied to prove Proposition 2.

Lemma 1. Let $m, n \in N$ and let $S = \{a_1, a_2, ..., a_m\}$ and $T = \{b_1, b_2, ..., b_n\}$ be two sets of vectors. If L is a lattice generated by the vectors in S and if T is equivalent to S with respect to integer linear combinations, then T is also a set of generators of the lattice L.

Proof of Lemma 1. Because the lattice L is generated by the vectors in S, we have

$$L = \{k_1 \bullet a_1 + k_2 \bullet a_2 + ... + k_m \bullet a_m : k_1, k_2, ..., k_m \in Z\} \quad (1)$$

Because S and T are equivalent with respect to integer linear combinations, for each $i \in \{1, 2, ..., n\}$, the vector b_i is an integer linear combination of a_1, a_2, …, and a_m. By Equation 1, we have $b_i \in L$.

On the other hand, for any vector $x \in L$, Equation 1 implies that there exist integers k_1, k_2, …, and k_m such that

$$x = \sum_{i=1}^{m} k_i \bullet a_i \quad (2)$$

For each $i \in \{1, 2, ..., m\}$, because a_i is an integer linear combination of vectors in the set T, there exist integers $l_{i,1}$, $l_{i,2}$, ..., and $l_{i,n}$ such that

$$a_i = \sum_{j=1}^{n} l_{i,j} \bullet b_j \quad (3)$$

By combining Equations 2 and 3, we have $x = \sum_{j=1}^{n} \left(\sum_{i=1}^{m} k_i \bullet l_{i,j} \right) b_j$. Hence x is an integer linear combination of b_1, b_2, …, and b_n. Thus T is also a set of generators of the lattice L.

Proposition 2. FCCL = recBCCL.

Proof of Proposition 2. The *recBCC* lattice shown in the right side of Figure 6 is generated by $v_1 = k \bullet (2, 0, 0)$, $v_2 = k \bullet (0, 2, 0)$, and $v_3 = k \bullet (1, 1, \sqrt{2})$ for some scaling factor $k > 0$. It is easy to check that those three vectors have the same length, v_1 and v_2 are orthogonal, and the angle between v_i and v_3 is 60° for each $i = 1, 2$. Let $b_1 = v_1 = k \bullet (2, 0, 0)$, $b_2 = -v_2 + v_3 = k \bullet (1, -1, \sqrt{2})$, and $b_3 = v_3 = k \bullet (1, 1, \sqrt{2})$. Then the two sets $\{v_1, v_2, v_3\}$ and $\{b_1, b_2, b_3\}$ are equivalent with respect to integer linear combinations. Because the three vectors b_1, b_2, and b_3 have the same length and the angle between any two of them is 60°, they generate an FCC lattice. Therefore, by Lemma 1, we have FCCL = recBCCL.

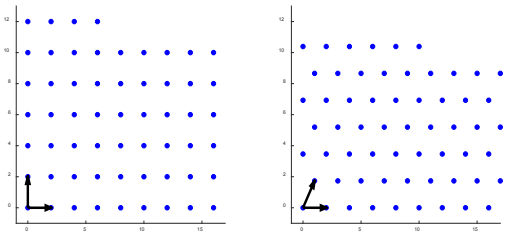

Figure 7. One level of an FCC lattice generated by two different sets of generators $\{v_1, v_2, v_3\}$ and $\{b_1, b_2, b_3\}$,respectively. The left shows a square lattice generated by v_1 and v_2; and the right shows a hexagonal lattice generated by b_1 and b_2

DOI: https://doi.org/10.30564/jcsr.v1i2.641

4. Possible Applications of the Rectangular Body Centered Cuboid Packing Lattices

In [14] by Biswas and Bhowmick, cubes are used to build a spherical object approximately. Because FCC and BCC lattices have certain advantages over simple cubic lattices, for some geometric objects, the discretization effect using those optimal sampling lattices may be better than the discretization effect using the corresponding Cartesian lattices. In the following, we introduce Hausdorff distance and use it to verify the discretization effects using different sampling lattices. For any $a,b\in R^n$, let $d(a,b)$ denote the distance between a and b; and let A and B be two nonempty subsets of R^n. In the following, Sup and Inf denote the supremum and infimum respectively. For each $a\in A$ let $d(a,B)=Inf\{d(a,b):b\in B\}$. Let $d(A,B)=Sup\{d(a,B):a\in A\}$. As in [15] by Zheng, the Hausdorff distance between A and B is $h(A,B):=\max\{d(A,B),d(B,A)\}$, and measures how far are A and B from each other.

To visualize the discretization effects easily, we first show a 2-dimensional example. Let Ω be the elliptic region $\left\{(x,y)\in R^2 \mid \frac{x^2}{35^2}+\frac{y^2}{8^2}\le 1\right\}$, and let $\tilde{\Omega}=\left\{(x,y)\in R^2 \mid \frac{x^2}{35^2}+\frac{y^2}{8^2}=1\right\}$ which is the boundary of Ω. The ellipse $\tilde{\Omega}$ is shown in red color in the subfigures of Figure 8. The top of Figure 8 shows the discretization of Ω using the Cartesian lattice generated by the two vectors $(2,0)$ and $(0,2)$. The bottom of Figure 8 shows the discretization of Ω using the hexagonal lattice generated by the two vectors $c\bullet\left(\frac{\sqrt{3}}{2},\frac{1}{2}\right)$ and $c\bullet\left(-\frac{\sqrt{3}}{2},\frac{1}{2}\right)$ where $c=\sqrt{\frac{8}{\sqrt{3}}}$. Because the area of a Voronoi cell for both the Cartesian and hexagonal lattice is 4, the resolution of sampling the elliptic region Ω using the Cartesian lattice is the same as that using the hexagonal lattice. Let C and H denote the sets consisting of all the sampled points of the region Ω using the Cartesian lattice and the hexagonal lattice, respectively. We may assume that $C\subseteq\Omega$ and $H\subseteq\Omega$ as usual. Hence $d(C,\Omega)=0$ and $d(H,\Omega)=0$. These two equations imply that $h(C,\Omega)=d(\Omega,C)$ and $h(H,\Omega)=d(\Omega,H)$. Because $C\subseteq\Omega$ and $\tilde{\Omega}$ is the boundary of Ω, we have $d(\Omega,C)=d(\tilde{\Omega},C)$. Similarly $d(\Omega,H)=d(\tilde{\Omega},H)$. To get the approximate values of $d(\tilde{\Omega},C)$ and $d(\tilde{\Omega},H)$, we discretize $\tilde{\Omega}$ using the scheme $x=a\bullet\cos(\theta)$ and $y=b\bullet\sin(\theta)$ with $\theta\in[0,2\pi)$ taking step size $\frac{\pi}{400}$. Let $\tilde{\Omega}_S$ denote the set consisting of these samples, i.e.,

$$\tilde{\Omega}_S=\left\{(a\bullet\cos(\theta),\, b\bullet\sin(\theta)) \mid \theta=0:\frac{\pi}{400}:\frac{799\pi}{400}\right\}.$$

The computations turn out that $d(\tilde{\Omega}_S,C)=2.2004$ and $d(\tilde{\Omega}_S,H)=2.0462$. Because of the small step size of θ, the set $\tilde{\Omega}_S$ well represents $\tilde{\Omega}$ in the comparison of $d(\tilde{\Omega},C)$ and $d(\tilde{\Omega},H)$. Hence $d(\tilde{\Omega}_S,H)<d(\tilde{\Omega}_S,C)$ implies that $d(\tilde{\Omega},H)<d(\tilde{\Omega},C)$. Therefore $h(H,\Omega)<h(C,\Omega)$, which means that H represents Ω better than C does. In other words, the hexagonal sampling is better than the corresponding Cartesian sampling for this 2-dimensional elliptic region.

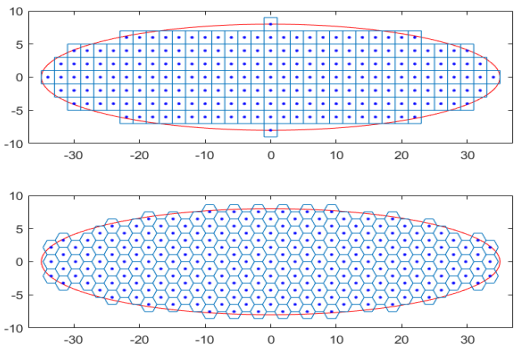

Figure 8. Discretization of an elliptic region. The top shows its discretization using a Cartesian lattice and the bottom shows its discretization using a hexagonal lattice

Similarly, in the 3-dimensional case, let Ξ be the el-

lipsoid $\left\{(x,y,z)\in R^2 \mid \frac{x^2}{13^2}+\frac{y^2}{7^2}+\frac{z^2}{6^2}\le 1\right\}$ and let $\tilde{\Xi}=\left\{(x,y,z)\in R^2 \mid \frac{x^2}{13^2}+\frac{y^2}{7^2}+\frac{z^2}{6^2}=1\right\}$ which is the boundary of Ξ. Let P denote the set consisting of all the sampled points of the 3-dimensional region Ξ using the Cartesian lattice generated by the three vectors $(2,0,0)$, $(0,2,0)$, and $(0,0,2)$; and let Q denote the set consisting of all the sampled points of Ξ using the FCC lattice generated by the three vectors $2^{-}\bullet(2,0,0)$, $2^{\frac{1}{6}}\bullet(0,2,0)$, and $2^{\frac{1}{6}}\bullet(1,1,\sqrt{2})$ shown in Proposition 2. Those three vectors for the FCC lattice are convenient for computer algorithms to discretize Ξ. With the usual assumption that $P\subseteq\Xi$ and $Q\subseteq\Xi$, we have $h(P,\Xi)=d(\Xi,P)$ and $h(Q,\Xi)=d(\Xi,Q)$. Similar to the previous 2-dimensional case, we have $d(\Xi,P)=d(\tilde{\Xi},P)$ and $d(\Xi,Q)=d(\tilde{\Xi},Q)$. We discretize $\tilde{\Xi}$ as $\tilde{\Xi}_S$ where

$$\Xi=\left\{(a\bullet\cos(\theta)\bullet\cos(\phi),\ b\bullet\sin(\theta)\bullet\cos(\phi),\ c\bullet\sin(\phi)) \mid \theta=0:\frac{\pi}{200}:\frac{399\pi}{200},\ \phi=-\frac{\pi}{2}:\frac{\pi}{200}:\frac{99\pi}{200}\right\}$$

The computations turn out that $d(\tilde{\Xi}_S,P)=2.2343$ and $d(\tilde{\Xi}_S,Q)=2.1641$. Because of the small step size of θ and ϕ, the set $\tilde{\Xi}_S$ well represents $\tilde{\Xi}$ in the comparison of $d(\tilde{\Xi},P)$ and $d(\tilde{\Xi},Q)$. Hence $d(\tilde{\Xi}_S,Q)<d(\tilde{\Xi}_S,P)$ implies that $d(\tilde{\Xi},Q)<d(\tilde{\Xi},P)$. Therefore $h(Q,\Xi)<h(P,\Xi)$, which means that the sampling effect using the FCC lattice is better than the effect using the corresponding Cartesian lattice.

Because $FCCL$ is the same as $recBCCL$, if we use the Voronoi cells of an FCC lattice (as in Figure 6 of in [13] by Zheng and Gu) to build an object, then a rectangular body-centered cuboid packing lattice may be considered for the convenience of machine operations or scientific computations as we have applied it for efficient algorithms discretizing the ellipsoid Ξ.

In the proof of Proposition 2, both $\{v_1,v_2,v_3\}$ and $\{b_1,b_2,b_3\}$ are sets of generators of the $recBCC$ lattice. Since v_1 and v_2 are perpendicular and have the same length, they generate a square lattice. When a machine lays spheres in one layer, usually a new sphere touches two previous spheres as shown in the left side of Figure 7. Because b_1 and b_2 generate a hexagonal lattice, when a machine lays spheres in one layer, a new sphere usually touches three previous spheres as shown in the right side of Figure 7.

Because the $recBCC$ lattice in Figure 5 is just a vertical stretch of the BCC lattice in Figure 4 by a scaling factor of $\sqrt{2}$, for any $recBCC$ lattice, there exists a BCC lattice and a direction such that the $recBCC$ lattice is just a vertical stretch of the BCC lattice by a scaling factor of $\sqrt{2}$. Because $\mathrm{FCCL}=\mathrm{recBCCL}$, for any FCC lattice, there exists a BCC lattice and a direction such that the FCC lattice is just a vertical stretch of the BCC lattice by a scaling factor of $\sqrt{2}$. Hence some algorithms for BCC lattices may be generalized to FCC lattices. FCC lattices and BCC lattices are applied in areas such as crystal systems as shown in Wikipedia page [11]. Because FCC lattices are the same as $recBCC$ lattices, the relation between BCC lattices and $recBCC$ lattices may help the study of related crystal systems.

5. Summary

We have studied several important 3-dimensional sphere packing ways and related lattices. The generators of those lattices are useful to show some relations and properties among those lattices. We have shown that FCC lattices are the same as $recBCC$ lattices. Hence an FCC lattice is a stretched structure of a BCC lattice in one direction. We have also shown that the FCC lattices may achieve better discretization effect for some geometric objects. Those results may have applications in the related areas.

References

[1] K. Ikeda and K. Murota. Bifurcation theory for hexagonal agglomeration in Economic Geography, Springer, Japan, 2014.

[2] A. Vince and X. Zheng. Arithmetic and Fourier transform for the PYXIS multi-resolution digital Earth model. Int. J. Digit. Earth, 2009, 2(1): 59–79.

[3] P. Hofmann and D. Tiede Image. Image segmentation based on hexagonal sampling grids. South-Eastern European Journal of Earth Observation and Geomatics, 2014, 3(2S): 173-177.

[4] Y. Wei, X. Li, J. Wang, C. Zhang, and Y. Liu. Graph cuts image segmentation in a hexagonal-image processing framework. Journal of Computational Information Systems, 2012, 8(14): 5953-5960.

DOI: https://doi.org/10.30564/jcsr.v1i2.641

[5] U. D. Burdescu, D. C. Ebânca, and F. Slabu. Graph-Based Segmentation Methods for Planar and Spatial Images. International Journal of Computer Science and Applications, 2015, 12(2): 120 – 143.

[6] K. Mostafa and I. Her. An Edge Detection Method for Hexagonal Images. International Journal of Image Processing, 2016, 10(4): 161-173.

[7] D. Van De Ville, T. Blu, M. Unser, W. Philips, I. Lemahieu, and R. Van de Walle. Hex-splines: A novel spline family for hexagonal lattices. IEEE Transactions on Image Processing, 2004, 13(6): 758–772.

[8] M. Mirzargar and A. Entezari. Voronoi splines. IEEE Transactions on Signal Processing, 2010, 58(9): 4572-4582.

[9] Li Xiangguo. Implementation of a simulated display for hexagonal image processing. Displays, 2017, 50: 63-69.

[10] Wikipedia. Sphere packing. Available online at http://en.wikipedia.org/wiki/Sphere_packing (accessed 18 March 2019)

[11] Wikipedia. Cubic crystal system. Available online at http://en.wikipedia.org/wiki/Cubic_crystal_system (accessed 18 March 2019)

[12] M. Kim, A. Entezari and J. Peters. Box Spline Reconstruction on the Face-Centered Cubic Lattice. IEEE Transactions on Visualization and Computer Graphics (Proceedings Visualization / Information Visualization), 2008, 14, (6): 1523-1530.

[13] X. Zheng, and F. Gu. Fast Fourier transform on FCC and BCC lattices with outputs on FCC and BCC lattices respectively. J. Math. Imaging Vis., 2014,49(3): 530-550.

[14] R. Biswas and P. Bhowmick. Layer the Sphere. The Visual Computer, 2015, 31: 787-797.

[15] X. Zheng. Box-counting dimension related to the boundary of hexagonal arrays for an efficient digital earth model. Fractals, 2010, 18(2): 223–233.

 DOI: https://doi.org/10.30564/jcsr.v1i2.641